The ISME Journal (2014) 8, 1175–1185

www.nature.com/ismej

ORIGINAL ARTICLE

Ecogenomic sensor reveals controls on N_2-fixing microorganisms in the North Pacific Ocean

Julie C Robidart[1,2,3], Matthew J Church[3,4], John P Ryan[2], François Ascani[3,4], Samuel T Wilson[3,4], Deniz Bombar[1,3], Roman Marin III[2], Kelvin J Richards[3,4], David M Karl[3,4], Christopher A Scholin[2,3] and Jonathan P Zehr[1,3]

[1]*Department of Ocean Sciences, University of California Santa Cruz, Santa Cruz, CA, USA;* [2]*Monterey Bay Aquarium Research Institute, Moss Landing, CA, USA;* [3]*Center for Microbial Oceanography: Research and Education, University of Hawaii, Honolulu, HI, USA and* [4]*Department of Oceanography, University of Hawaii, Honolulu, HI, USA*

Nitrogen-fixing microorganisms (diazotrophs) are keystone species that reduce atmospheric dinitrogen (N_2) gas to fixed nitrogen (N), thereby accounting for much of N-based new production annually in the oligotrophic North Pacific. However, current approaches to study N_2 fixation provide relatively limited spatiotemporal sampling resolution; hence, little is known about the ecological controls on these microorganisms or the scales over which they change. In the present study, we used a drifting robotic gene sensor to obtain high-resolution data on the distributions and abundances of N_2-fixing populations over small spatiotemporal scales. The resulting measurements demonstrate that concentrations of N_2 fixers can be highly variable, changing in abundance by nearly three orders of magnitude in less than 2 days and 30 km. Concurrent shipboard measurements and long-term time-series sampling uncovered a striking and previously unrecognized correlation between phosphate, which is undergoing long-term change in the region, and N_2-fixing cyanobacterial abundances. These results underscore the value of high-resolution sampling and its applications for modeling the effects of global change.

The ISME Journal (2014) **8,** 1175–1185;doi:10.1038/ismej.2013.244; published online 30 January 2014
Subject Category: Microbial population and community ecology
Keywords: autonomous sensing; biosensors; diazotrophs; microbial oceanography; nitrogen fixation; time-series

Introduction

Nitrogen (N_2)-fixing microorganisms are important sources of new nitrogen (N) in N-limited ocean regions worldwide (Carpenter and Capone, 2008), and are responsible for sustaining a large fraction of carbon export from surface waters to depth in major ocean basins (Karl *et al.*, 2012). Molecular tools to quantify these organisms have become available in recent years; however, such tools typically rely on traditional oceanographic ship-based sampling and their application is thus limited. New developments using *in situ* chemical sensing and continuous time-series export sampling in the oligotrophic open ocean have demonstrated the importance of episodic events in modulating marine biogeochemical cycles (Johnson *et al.*, 2010; Karl *et al.*, 2012; Ascani *et al.*, 2013), but the variety of processes we can sample and sense continuously at the microbial level *in situ* is extremely limited. As a result it has been difficult to determine how ephemeral environmental fluctuations control the growth and activities of N_2-fixing microbes and how such fluctuations might be used to gain a perspective of how longer-term trends such as global environmental change will impact these keystone species.

The development of 'ecogenomic sensors' (Preston *et al.*, 2011) has in part been driven by this challenge of enabling autonomous, high-resolution quantification of microbial nucleic acids *in situ*. In this study we deployed one of these devices, the Environmental Sample Processor (ESP; Figure 1d; Scholin, 2013), with coupled physical and biogeochemical sensors on a drifter near the long-term biogeochemical time-series Station ALOHA in the North Pacific Subtropical Gyre. Our objective was to determine the scales at which N_2-fixing microorganisms change and the environmental controls on their abundances. The resulting data sets reveal links that are important to predicting the abundances of N_2-fixing microorganisms with respect to long-term changes in nitrogen and phosphorus concentrations, such as those that have been documented at Station ALOHA (Karl *et al.*, 2001).

Correspondence: JC Robidart, Department of Ocean Sciences, University of California Santa Cruz, 1156 High Street, Santa Cruz, CA 95064, USA.
E-mail: jrobidart@ucsc.edu
Received 20 August 2013; revised 28 November 2013; accepted 2 December 2013; published online 30 January 2014

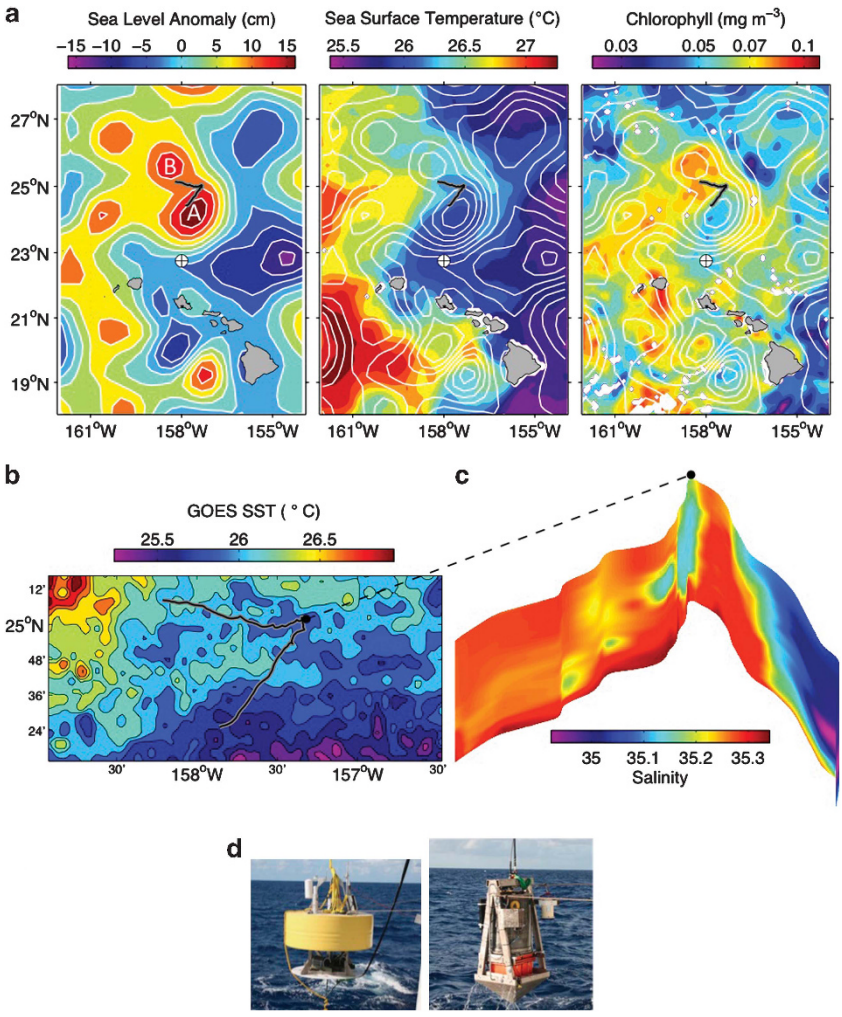

Figure 1 BioLINCS environmental setting. (**a**) Sea-level anomaly (SLA: contours overlaid on all panels), sea surface temperature (SST) and near-surface chlorophyll concentrations are averages of satellite data from AVISO (Archiving, Validation and Interpretation of Satellite Oceanographic data) and MODIS (Moderate Resolution Imaging Spectroradiometer) Aqua, for 6–20 September 2011. The gray/black track shows the drift path of the instrumented platform (ESP, CTD and Acoustic Doppler Current Profiler (ADCP)), which began at the southernmost point. SLA image depicts eddies A and B, which influenced the ESP drift trajectory and are described in the text. The clockwise circulation of eddy A and associated stirring of regional water types is evident in the SST and chlorophyll patterns. Station ALOHA is marked by the circle + symbol. (**b**) GOES (Geostationary Operational Environmental Satellites) SST from 12–13 September 2011 (nighttime). (**c**) Salinity along the ESP drift track, upper 80 m. (**d**) ESP drifter float (left) and base (right) are connected via an electromechanical cable. The ESP is sealed within the cylindrical pressure housing mounted to the platform base.

Materials and methods

ESP preparation

During an oceanographic research cruise aboard the *R/V Kilo Moana* from 6–21 September 2011 (KM 11–25, BioLINCS: Biosensing Lagrangian Instrumentation and Nitrogen Cycling Systems), intensive sampling for microbial abundances and activities was conducted within the North Pacific Subtropical Gyre using autonomous instrumentation and shipboard sampling. The ESP was deployed on a drifting platform as described previously (Ottesen *et al.*, 2013) with an Acoustic Doppler Current Profiler and conductivity-temperature-depth sensor (CTD) mounted to the ESP base. The ESP was fitted with quantitative PCR (qPCR) reagents for detecting *nifH* genes from *Trichodesmium*, *Candidatus* Atelocyanobacterium (referred to as 'Atelocyanobacterium' in this text; Thompson *et al.*, 2012) and *Crocosphaera*, and qPCR reaction conditions and kinetics were validated in the laboratory before deployment (as in Preston *et al.*, 2011; Robidart *et al.*, 2012; Supplementary Table 1). The ESP was maintained in an air-conditioned room until deployment and qPCR standard curves were verified on recovery of the instrument to check reagent stability and instrument calibration. The assay for *Crocosphaera* failed this post-recovery standard curve check and is not included in analyses presented here. Changes in the bacterioplankton community composition were also measured on the ESP using ribosomal RNA probes in a sandwich hybridization array format to

Table 1 Microbial population patchiness as measured by ESP

	Ratio most:least abundant	
	ESP	*Ship*
	Array ($n=15$)	FCM ($n=9$)
Prochlorococcus	2.53	1.31
Synechococcus		1.92
Picoeukaryotes	N/A	1.74
Heterotrophs*	2.15	1.10
	qPCR ($n=14$)	qPCR ($n=16$)
5-m Depth *Atelocyanobacterium*	NA	176.86
25-m Depth *Atelocyanobacterium*	792.59	627.56
45-m Depth *Atelocyanobacterium*	NA	1636.43
75-m Depth *Atelocyanobacterium*	NA	48.45
Trichodesmium	217.75	32.38
Crocosphaera	NA	37.04
Gamma proteobacteria	>19.32	>8.93
Richelia-Rhizosolenia symb.	NA	>13.22
Richelia-Hemialus symb.	NA	>8.57
Synechococcus II, cluster 1	NA	20.14
Synechococcus II, cluster 2	NA	2.5
Synechococcus III	NA	6.6

Abbreviations: CTD, conductivity-temperature-depth sensor; ESP, Environmental Sample Processor; FCM, flow cytometry; N/A, no data were collected for these parameters; qPCR, quantitative PCR. Patchiness measured by ESP (15 sandwich hybridization array samples and 14 qPCR samples) and from ship-collected CTD niskin samples (flow cytometric (FCM) and qPCR samples, 9 each) at 25 m depth unless stated otherwise. For qPCR abundances, '>' means that the lower gene counts were below the limit of quantification (five copies) for these targets. Variation in diazotroph populations well exceeds variation in other cyanobacteria populations, as well as in picoeukaryotes and 'heterotrophs'. *Heterotrophs are defined as SAR11, SAR86 and marine Roseobacter clades for hybridization array (probes described in Preston *et al.*, 2009), and as all non-fluorescing microbes for flow cytometry counts.

detect Bacterial and Archaeal clades from a bulk sample lysate as described previously (Preston *et al.*, 2009; Table 1). Spot intensity of each hybridization probe (an average of eight spotted probes per target) were background subtracted and changes in the picoplankton community were calculated based on relative sample-to-sample variation in spot intensity for each target over time.

Shipboard sample collection

Aboard the ship, discrete seawater samples were collected from CTD rosette bottles fired at 5, 25, 45, 75, 100, 125, 150, 175 and 200 m near the ESP over the course of the cruise. Flow cytometric analyses and all biogeochemical measurements were performed according to the Hawaii Ocean Time-series (HOT) sample analytical protocols found at http://hahana.soest.hawaii.edu/hot/methods/results.html. For nucleic acid analyses, 2 l samples were collected from 25 ± 0.5 m at 12 stations (Supplementary Figure 1), filtered onto 0.22-μm Supor filters with a 10-μm pore size prefilter and immediately frozen in liquid nitrogen. Samples were shipped to the lab at the University of California at Santa Cruz and stored at $-80\,^{\circ}$C until processing.

Community analyses

DNA extractions were carried out in the lab as described (Moisander *et al.*, 2010) with a Qiacube (Qiagen, Germantown, MD, USA) to carry out the column-based extraction portion of the protocol according to the manufacturer's instructions.

Lab-based qPCR was carried out using Taqman Gene Expression Master Mix (Life Technologies, Carlsbad, CA, USA) and with optimized assay conditions as in Supplementary Table 1. *Synechococcus phnD* gene assays were developed and optimizations were performed with Accuprime qPCR mix (Life Technologies) with an added 2.5 mM $MgCl_2$ per 30 μl reaction. Cross-reactivity tests were performed between each *Synechococcus* cluster (Clade II clusters 1 and 2, and Clade III) and all assays were specific to their targets at concentrations above 10 copies per reaction (Supplementary Figure 7). Non-target clade concentrations were not high enough to change gene quantifications over this time series for any of the assays. *phnD* is present as one copy per genome in sequenced genomes from different clades of *Synechococcus*, and here we assume this is the same for *Synechococcus* in the environment (Ilikchyan *et al.*, 2010).

Biogeochemical analyses

BioLINCS CTD rosette sampling collected samples from nine discrete depths in the upper ocean: 5, 25, 45, 75, 100, 125, 150, 175 and 200 m. For subsequent analyses of inorganic nutrients, 125–500 ml seawater was subsampled from the CTD rosette bottles into 125 or 500 ml acid-washed polyethylene bottles and frozen upright until nutrient analyses. On shore, high-sensitivity nutrient measurements were conducted from photic zone waters according to Karl and Tien (1992) and Dore and Karl (1996). Nutrients from the deeper samples were analyzed using a 6-channel Bran and Luebbe Autoanalyzer III as described in 'HOT Laboratory Protocols' (http://hahana.soest.hawaii.edu).

Remote sensing

Eddies and advective anomalies were described using sea-level anomaly (SLA) data from AVISO combined microwave and infrared sea surface temperature data from Remote Sensing Systems and surface chlorophyll data from MODIS Aqua (Figure 1). The life history of eddy A (trajectory and size of the eddy) was analyzed with a searching algorithm using a Gaussian SLA profile. Size is defined as the width of the Gaussian profile and depicted by the size of the red circles in Supplementary Figure 3. SLA for the Station ALOHA region for Supplementary Figure 4 were gathered and assembled from the Colorado Center for Astrodynamics Research (http://eddy.colorado.edu/ccar/ssh/hist_global_grid_viewer).

HOT data were obtained from the HOT Data Organization & Graphical System (http://hahana.soest.hawaii.edu/hot/hot-dogs/). Near-monthly *nifH* gene abundances measured at Station ALOHA from 2008 to 2011 were quantified according to Church *et al.* (2005, 2008). In this study, we define 'summer' as any time at which temperatures at 25 m depth exceeded 25.6 °C (corresponding with approximately 1 July–15 Nov, 138 days), and for comparability we define 'spring' as an equal number of days (in this case, 138) preceding 'summer' (that is, 13 February – 30 June). These dates roughly correspond with the official dates of each season, but we chose to place quantitative restraints on the dates in order to compensate for interannual differences.

Results

High-resolution Lagrangian sampling

The drifting ESP sampled every 16 h over a 10-day period (7–16 September 2011) ~160 km north of Station ALOHA (Figure 1a). In this region, eddy-forced advection is evident as the anticyclonic wrapping of relatively warm, chlorophyll-enriched water around eddy A (Figure 1a). The warm filament along the northern periphery of eddy A is the most pronounced signature of this advection, indicating eastward flow in that area. A westward counterflow between eddy A and eddy B is suggested by the westward deflection of sea surface temperature isotherms in that region, corresponding with the westward transport of the ESP. Lateral mixing between the eddy-stirred water types is indicated by the patchiness evident in the higher resolution and more synoptic sea surface temperature (Figure 1b), and by water column salinity along the drift track (Figure 1c).

The ESP quantified N_2-fixing microorganism nitrogenase (*nifH*) gene abundances by qPCR assays. The instrumented autonomous platform (ESP, Acoustic Doppler Current Profiler and CTD) sampled within the upper mixed layer at 24 m depth, drifting northeastward for 6 days before turning west for the final transit (Figure 1). The ESP drift track relative to satellite altimetry indicates that the instrument sampled within the eddy periphery while traveling northeastward (eddy A, Figure 1a). Salinity and temperature averaged 35.19 ± 0.09 and 26.09 ± 0.20 °C, respectively, during this drift period (Figure 2).

The abundances of diazotrophs (as inferred from qPCR *nifH* gene quantifications) differed between the various genera of N_2-fixing bacteria, including the unicellular cyanobacterium genus Atelocyanobacterium, the filamentous cyanobacterium *Trichodesmium* and an uncultivated *nifH*-gene-containing group of proteobacteria (Church *et al.*, 2005). *Trichodesmium* abundances were extremely patchy, with a 140-fold increase during one period of 32 h and 30 km during the first portion of the *in situ* experiment and a 218-fold decrease during a 32 h and 29 km observation period near the end of the instrument drift (Figure 3b). The maximum *Trichodesmium nifH* abundances in our study are among the highest reported near Station ALOHA since 2005 (Fong *et al.*, 2008; Figure 3a). Surprisingly, the unicellular *Atelocyanobacterium* were also abundant, and despite the quasi-Lagrangian nature of drifter sampling, even more variable than *Trichodesmium* abundances, fluctuating by nearly three orders of magnitude in *nifH* copies (from 4.3×10^2 to 2.4×10^5) per liter over one 32-h, 22-km drift period (Figure 3b).

Shipboard verification of ESP qPCR abundances

ESP-measured diazotroph abundances were confirmed by samples collected using the ship's CTD rosette system (Figure 2d), which was deployed <6 km from the ESP (with most samples taken <1 km from the ESP; Supplementary Figure 1). The patterns of *Trichodesmium* abundances determined from shipboard sampling were generally similar to those observed by the ESP, with high variability in abundances occurring over the first 3 days of the deployment. Although shipboard *Trichodesmium* abundance measurements were the same order of magnitude as the abundances reported by the ESP, they were less variable, with a 32-fold ($n = 9$) change in density over the sampling period relative to 218-fold change observed using the ESP ($n = 14$; Table 1). This discrepancy is likely due to the heterogeneous distributions of *Trichodesmium* and the higher frequency of ESP sampling. The extraordinary patchiness in these samples is illustrated by an eightfold change in *Trichodesmium* concentration over a single 7-km, 13-h span. The patterns of Atelocyanobacterium densities as determined by shipboard sampling were also similar to those obtained by the ESP overall, with high variability, ranging from 2.1×10^2 to 5.3×10^4 *nifH* copies per liter over a single 26-km, 24-h period (Figure 2d).

The ESP ribosomal RNA abundance patterns for several dominant, non-N_2-fixing microbial groups, including *Prochlorococcus*, *Synechococcus* and picoplanktonic heterotrophs (Preston *et al.*, 2009), were used to evaluate heterogeneity in the broader population. In contrast to the diazotrophs, the concentrations of these prokaryotes were relatively constant, varying <2.5-fold over the entire deployment (Table 1). Flow cytometric quantifications of *Prochlorococcus*, *Synechococcus*, picoeukaryotes and heterotrophs supported the population stability observed using the ESP probe arrays (Table 1). The maximum variation by ship-based flow cytometry was in the *Synechococcus* population, which varies by a factor of only 1.92. In stark contrast, patchiness in diazotroph populations far exceeded that of these other groups of microbes, with the lowest degree of variation in the *Trichodesmium* population, with a 32-fold degree of variation in *nifH* qPCR abundance (Table 1). For all diazotrophs, this measured

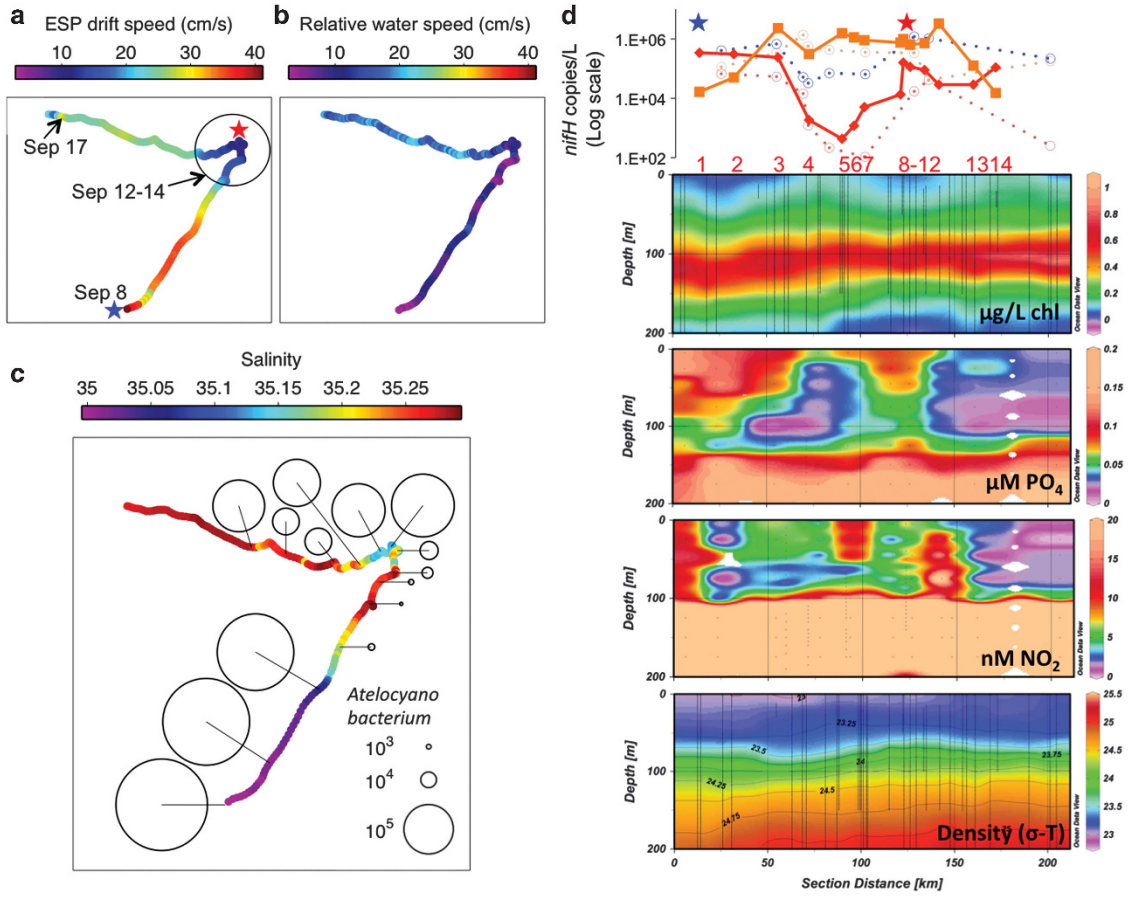

Figure 2 ESP drift contours of nutrient concentrations and ecological observations. (**a**) Platform velocity (speed in color, direction in track). Earth-referenced velocity of the ESP was determined from the time series of its GPS position. (**b**) Platform quasi-Lagrangian behavior based on the ESP-relative speed of water 3 m above the ESP. A water velocity of zero indicates Lagrangian movement (that is, perfect movement with the currents). (**c**) Salinity, with abundances of Atelocyanobacterium (in *nifH* gene copies per l). (**d**) Atelocyanobacterium are in red, *Trichodesmium* in orange and *Crocosphaera* in blue, plotted relative to the cruise transit distance. Solid lines indicate ESP-collected data and dotted lines are data from seawater collected from CTD niskins on board the ship. Diazotroph abundances are in agreement between the ESP and CTD. Chlorophyll, phosphate, nitrite and density are plotted versus depth and transit distance for this same period. Phosphate concentrations in surface waters are high but variable during the cruise. Relatively high nitrite concentrations extend from depth to the surface waters in the eastern portion of the inter-eddy transition zone, as the ESP circled twice due to contrasting currents. Numbers in red indicate ESP sample numbers (samples taken 16 h apart), corresponding with locations in Supplementary Figure 1. Stars indicate regions of lowest SLA sampled, where nutrients are highest in the surface waters. The red star in **a** and **d** also corresponds with the apex of the ESP transit.

population heterogeneity (maximum/minimum abundace) was at least 16 times higher than that of other measured microbial populations.

In order to determine whether this heterogeneity was specific to N_2-fixing microorganisms or more generally represented fluctuations in phylogenetically constrained groups (the *nifH* targets specific, low-abundance genera while more broadly characterized taxa are identified by flow cytometry and ribosomal RNA hybridization probes), we also quantified *phnD* gene abundances of three clades of *Synechococcus* that have similar abundances to the diazotrophs (on the order of 10^5 cells per l at 25 m depth). These clades varied by a maximum of 20-fold (<10% and 3% of the observed variability in *Trichodesmium* and Atelocyanobacterium, respectively) during the 10-day sampling period (Table 1). Diazotroph populations were more heterogeneous than populations of clades of cyanobacteria with similar abundances.

We compared our data with several years of summertime N_2-fixing cyanobacteria abundances measured at Station ALOHA (Figure 3). Although populations did not decrease to below detection limits during the BioLINCS cruise, observed changes in abundances during this quasi-Lagrangian time series were comparable to the range of summertime patchiness detected over all measured (three to six in total) summers at Station ALOHA for two of the three nitrogen-fixing cyanobacteria (Figure 3).

Relationships between diazotroph abundances and ocean biogeochemistry

Abundances of N_2-fixing microbes correlated strongly with salinity (Atelocyanobacterium

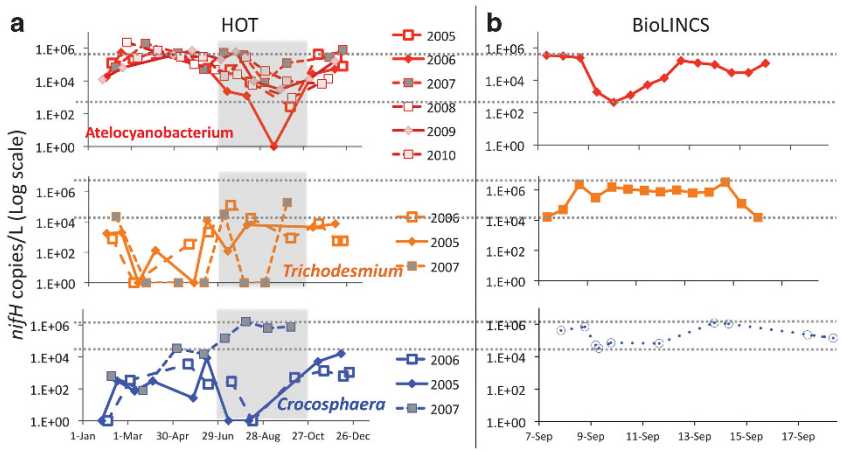

Figure 3 Time series for the three most abundant diazotrophs during the present study and historical observations from Station ALOHA. (**a**) Atelocyanobacterium, *Trichodesmium* and *Crocosphaera* abundances over 3 to 6 years of monthly sampling at Station ALOHA (2008–2011). Summer months are darkened in gray. (**b**) Abundances of the same organisms during BioLINCS. See Supplementary Figure 3 for physical orientation by ESP sample number. Dotted lines delineate the range of abundances quantified during BioLINCS, demonstrating a heterogeneity in the Atelocyanobacterium and *Trichodesmium* populations that is comparable to the 3 years of summer patchiness data from ALOHA.

Pearson's R-value $= -0.91$, $P<0.05$, $n=14$), despite high population heterogeneity. The significant, negative correlation between salinity and phosphate (Pearson's correlation $R=0.99$, $P<0.05$, $n=8$) translates to a significant positive correlation between Atelocyanobacterium abundances and calculated phosphate concentrations (using ESP-coupled CTD salinity: (phosphate) $=((-0.371\times$ salinity$)+13.09)$ along the western edge of eddy A ($R=0.91$, $P<0.05$; $n=14$, Figure 4, Supplementary Figure S2)). The Acoustic Doppler Current Profiler mounted on the ESP revealed that the drifting instrument was largely moving with the currents, in terms of direction and speed, during this phase of the transit (Figure 2 and 'Drifter behavior' in Supplementary Information).

Shipboard CTD-collected samples showed that the unicellular N_2-fixing cyanobacterium *Crocosphaera watsonii* was abundant relative to historic records and showed a weaker, but similar trend to Atelocyanobacterium, with higher abundances in lower salinity and higher phosphate waters along the western portion of eddy A (Pearson correlation $R=0.71$, $P=0.05$, $n=8$; Figure 4). Excluding two outlier observations that we attribute to the patchiness of *Trichodesmium* tufts, *Trichodesmium* and *Crocosphaera* were negatively correlated over this time (Pearson correlation $R=-0.94$, $P<0.05$, $n=10$ of 12 samples; Figure 4d), and *Trichodesmium* had similar patchy distributions. Depth profiles of Atelocyanobacterium from samples collected from 5 and 45 m depths mimicked the patchiness at 25 m, revealing a vertical component to the Atelocyanobacterium population, with heterogeneity over the >100 km transit extending to at least 45 m depth (Table 1).

Analyses of historical HOT data revealed a significant negative correlation between phosphate concentrations and salinity for samples collected since 2008 (Pearson correlation $R=-0.86$, $P<0.05$, $n=8$). Moreover, we found a significant positive relationship ($R=0.87$, $P<0.05$, $n=8$) between Atelocyanobacterium abundances and phosphate concentrations during the summer months (Figure 4), but no significant relationship between Atelocyanobacterium and salinity was observed for the period 2008–2012.

Bioavailable Fe may also be a limiting nutrient for diazotroph abundances (Sohm *et al.*, 2011; Shilova *et al.*, 2014). Although we did not measure Fe concentrations during this cruise, it is plausible that Fe covaried with phosphate, leading to the observed phosphate-to-diazotroph trends. However, Fe is often present in sufficient concentrations at Station ALOHA (Boyle *et al.*, 2005) and we recognize that the phosphate-to-iron correlation would have to be quite strong to lead to the observed R-values in this study (which is certainly possible, as Fe also comes from depth in this region).

Analysis of mesoscale eddies

Since 1989, 8 of the 10 highest recorded summer phosphate concentrations collected from 25 m depth as part of the HOT monthly sampling program (not including those from BioLINCS) were associated with positive SLA (anticyclonic eddies; Supplementary Figure 4) and just one was in a region of negative SLA. The 10 highest concentrations of phosphate at Station ALOHA (1989–2012) had an average of 105 ± 17 nM (spring) and 116 ± 22 nM (summer; Supplementary Figure 5).

Discussion

Because of their low abundances in the marine environment, and because some cannot be identified precisely by microscopy or by remote sensing,

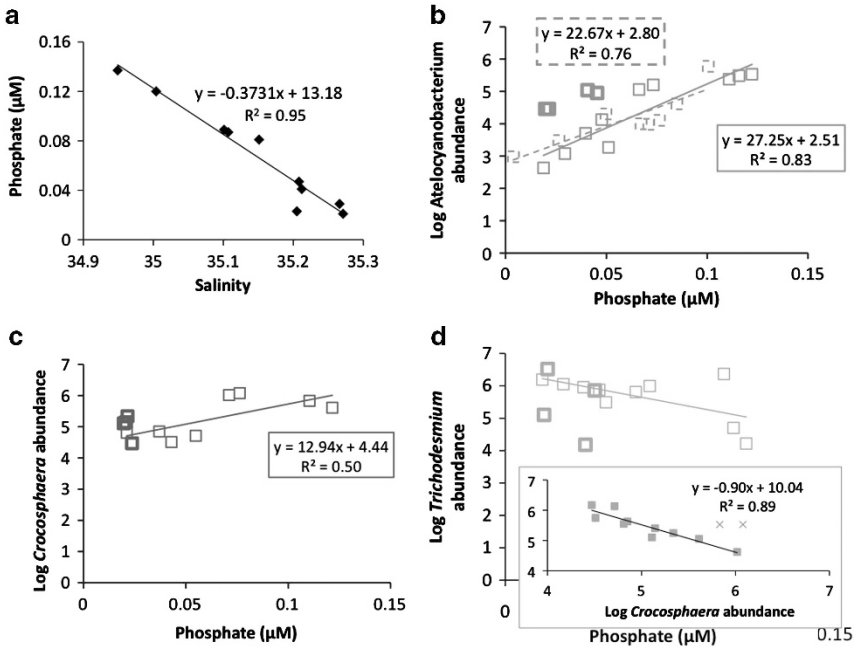

Figure 4 Regressions with phosphate. (**a**) The significant relationship between salinity and phosphate during the BioLINCS cruise allowed extrapolation of phosphate concentrations using salinity data, from ESP-collected samples. (**b**) Log of *Atelocyanobacterium* abundances versus phosphate concentrations. For remaining panels, squares correspond to BioLINCS eddy A samples, bold squares correspond with BioLINCS inter-eddy transition zone samples and dashed squares correspond with HOT data since 2008. The significant relationship between Atelocyanobacterium abundances and phosphate concentrations in the summer for all data sets since 2008 (note that here we show R^2-values, whereas Pearson's correlation R-values are reported in the main text). (**c**) Positive relationship between the log of *Crocosphaera* abundances and phosphate concentrations ($P=0.05$). (**d**) Negative relationship between the log of *Trichodesmium* abundance versus phosphate concentration ($P>0.05$). Inset shows the same log of *Trichodesmium* abundances versus *Crocosphaera* abundances ($R=-0.88$; $P<0.05$); 'X' designate the two outliers of this correlation. Abundances in the inter-eddy transition zone are elevated for the unicellular cyanobacteria, and depleted for *Trichodesmium*.

molecular approaches have proven valuable in identifying diazotroph distributions. Previous ship-based expeditions have successfully used this approach to quantify diazotrophs over multiple seasons (Langlois *et al.*, 2008; Church *et al.*, 2009; Foster *et al.*, 2009) and large geographic ranges (Langlois *et al.*, 2008; Moisander *et al.*, 2010). These studies demonstrate that nitrogen-fixing communities are patchy and can vary seasonally. Although diazotroph blooms recur every summer (White *et al.*, 2007; Dore *et al.*, 2008), the precise timing and location of blooms is unpredictable. Here we sought to use high-resolution, quasi-Lagrangian sampling to determine (1) whether the patchiness previously reported reflects spatial or temporal variability, and (2) whether abundances can be predicted within the summer and attributed to specific physical and/or chemical factors. Our drifter-based sampling program allowed us to address these objectives by confining the sampling regime to a specific season and depth, and at scales relevant to the target organisms (that is, within ephemeral current fields and during small-scale mixing events; Dickey 2003). This focused approach over a very short period of time surprisingly revealed a wide range of environmental conditions, typically encountered over the course of long-term time series and ship-based expeditions. Here the *quasi*-Lagrangian nature of the drift allowed us to capture microbial heterogeneity over both space and time, as evidenced by the range of salinities encountered.

Unexpected microbial heterogeneity revealed by high-resolution Lagrangian sampling

Over the BioLINCS ESP 10-day time series, variability in diazotroph concentrations (or nifH gene abundances per liter) was similar in magnitude to the variability in abundances (Fong *et al.*, 2008; Church *et al.*, 2009), despite quasi-Lagrangian sampling. The variability in diazotroph abundances was similar in magnitude to the variability in abundances seen over monthly time scales during the summer in previous years (Figure 3). Further, our results demonstrate that the abundances of N_2-fixing keystone species can display much greater spatiotemporal variability than other groups of microbes, including other members of the cyanobacteria (Table 1). These findings have implications for modeling the distributions of N_2-fixing organisms and rates of N_2-fixation in open ocean ecosystems. Although major population shifts have been documented for several metazoan keystone species (for example, Jackson *et al.*, 2001), as a result of the complexity of environmental variation on smaller scales, documenting the same for microbial

species has proven difficult unless the species are easily identifiable (such as *Trichodesmium*; Davis and McGillicuddy, 2006; Westberry and Siegel, 2006). Our results indicate that major population fluctuations of keystone microbial species occur on the order of days and kilometers, even when sampling in a quasi-Lagrangian manner (Figures 1 and 2).

Evaluation of controls on microbial distributions

The range in salinity encountered during the BioLINCS cruise (0.28) is large for the region, representing 87% of the summer range observed in HOT measurements conducted since 2009 and 28% of the full range for this region since 1989 (Lukas 2001; Lukas and Santiago-Mandujano, 2008). We observed robust relationships between diazotroph abundances and salinity over the course of the cruise (Supplementary Figure 6), highlighting how small spatiotemporal scale fluctuations in ocean physics have critical roles in controlling distributions and abundances of microbes on small scales. Moreover, the extreme heterogeneity observed during our study suggests that high-resolution sampling is the key to efficient resolution of the processes that govern diazotroph distributions and abundances within seasons. This population heterogeneity over small scales has important implications for how we assess the metabolic activities of diazotrophs and how we extrapolate from a limited number of measurements to larger ecosystem-level processes.

A combination of ship-based measurements, satellite SLA, finite-size Lyapunov exponent modeling and ocean color indicate that the high heterogeneity in physical and chemical conditions during BioLINCS is the result of both advection and mixing. A calculation of finite-size Lyapunov exponent (for example, Lehahn *et al.*, 2007) confirms mixing between eddies A and B during the period of sampling. The negative correlation between salinity and phosphate measured during this cruise demonstrates that Atelocyanobacterium was abundant within a localized current where salinity and temperature were low, but where phosphate was elevated relative to the surrounding waters. Atelocyanobacterium decreased in abundance as the high phosphate current mixed with adjacent waters within the eddy. This trend was also seen with *Crocosphaera* but was not observed for *Trichodesmium* or the 'N_2-fixing proteobacteria'.

Although the relationship between unicellular diazotroph abundances and salinity is not supported in the historic data from Station ALOHA, these microorganisms are positively correlated with phosphate in this region in the summer months since 2008 according to HOT data sets (Figure 4). Thus, it appears that lower nutrient concentrations can account for low abundances of unicellular diazotrophs during the summer. When combined with eddy-driven nutrient advection into the region year-round and the corresponding enhancement in unicellular diazotrophs, these organisms exhibit patchier distributions in the summer compared with other seasons.

Phosphate correlated with Atelocyanobacterium abundances more than any other measured parameter in this comprehensive data set. It must be noted that trace metals and vitamins are not routinely measured during HOT sampling, and it is possible that one of these factors parallels variations in phosphate. Nevertheless, these analyses establish the extent of natural variation and support a link to phosphate for this important diazotroph in the contemporary North Pacific Subtropical Gyre. This finding could be used as a basis to predict the fate of Atelocyanobacterium in modeled future ocean states.

Local enhancement of unicellular diazotrophs after a mixing event

In the westward transit during BioLINCS (the 'inter-eddy transition,' Figure 1), there were opposing currents, high but variable nutrients within the mixed layer and indications of diapycnal mixing. Mixing is apparent at the apex of the ESP drift, where nitrite concentrations are elevated from the nitrite maximum into the shallow photic zone (Figure 2d at 130–155 km) and density inversions occur (Supplementary Figure 2C). In this region, both Atelocyanobacterium and *Crocosphaera* had elevated abundances over what would be predicted based on the strong physics-driven correlations in eddy A. Linear correlations between diazotroph abundances and salinity, a conservative property of seawater, indicate that horizontal eddy stirring is the dominant driver of distributions along the northeastward transit. However, in the inter-eddy region the unicellular cyanobacterial diazotrophs (Atelocyanobacterium and *Crocosphaera* shown in Supplementary Figure 6) had elevated abundances (25.5-fold and 1.6-fold, respectively) relative to samples with the same salinity in eddy A. Such observations indicate locally enhanced growth and/or microbial accumulation (Guidi *et al.*, 2012) in the complex inter-eddy region despite a high temperature that is well above the predicted optimal for Atelocyanobacterium (Church *et al.*, 2009). In this area, *Trichodesmium* had $\sim$13-fold lower abundances than would be expected based on distributions relative to salinity in eddy A. Unlike the previously strong correlations with environmental factors, the inter-eddy region represents a complex congruence of factors that make diazotroph distributions unpredictable based on horizontal eddy stirring alone.

Anticyclonic eddies linked to surface phosphate concentrations

Twelve percent of the summer phosphate concentrations sampled since 1989 are below the

recorded historic spring minimum for the region (Supplementary Figure 5), presumably reflecting increased stratification during the summer months and lower vertical nutrient supply. Satellite altimetry and HOT measurements were used to determine whether the passage of mesoscale eddies through the ALOHA sampling region is a major source of biogeochemical variability in that time series. Indeed, the highest concentrations of recorded phosphate in the summer months were within mesoscale anticyclonic eddies, (Supplementary Figures 4 and 5B), which was unexpected. High stratification and lower background nutrient concentrations in surface waters during the summer amplify the importance of small nutrient increases in the upper ocean. Mesoscale eddies impart significant variability to ocean biogeochemistry at Station ALOHA (Church *et al.*, 2009) and the impacts of such events appear most pronounced during the summer, resulting in a larger range of phosphate concentrations in the photic zone over the summer months than other seasons. This extreme range of conditions has important implications for the growth and activities of microorganisms.

An excess of phosphate in the photic zone can be caused by: (1) recent delivery from depth, (2) accumulation due to low demand from the microbial community (that is, phosphate is not a limiting nutrient) or (3) a localized biological or atmospheric source of phosphate. Although we did not measure phosphate flux during the BioLINCS cruise, the strong salinity–phosphate relationship suggests a delivery of low-salinity, high-phosphate water into the region of sampling. During the HOT measurement period, there is also a high frequency (79%) of below-average salinity among the highest phosphate samples (Supplementary Figure 5B). Here, eleven of the fourteen highest-phosphate samples collected during summers from 25 m depth have salinities below the average for the HOT summer salinity dataset. While this may suggest a physical mechanism, lack of phosphate consumption has also been demonstrated in the region (Zehr *et al.*, 2007; Dore *et al.*, 2008).

A phosphate-stimulated increase in N_2 fixation activity would lead to a negative correlation between phosphate concentration and diazotroph abundance, as microbes deplete phosphate from nitrogen-limited seawater at steady state (that is, no external phosphate input). During BioLINCS, we observed the stirring of near-record high-phosphate seawater with very low-phosphate seawater. The positive correlation between the abundances of unicellular diazotrophs and phosphate likely reflects the mixing of waters where these organisms are nutrient limited (low abundance) versus those where they are nutrient repleted (high abundance). The positive correlation in historic HOT records, which reflect a variety of ocean states, was unexpected. Although the link with phosphate (and not salinity) is clear, we cannot yet fully explain the mechanism that leads to this correlation.

Implications

Marine microorganisms can display heterogeneity over time and space, and variations in diazotroph community composition are often associated with significant changes in N_2 fixation rates (Church *et al.*, 2009; Shiozaki *et al.*, 2013; Wilson *et al.*, 2013). Understanding the controls on distributions of microbial populations is crucial for predicting future changes in ocean biogeochemistry (Zehr *et al.*, 2011; Giovannoni and Vergin 2012). The BioLINCS cruise demonstrates the promise of next-generation autonomous *in situ* sensors for revealing such processes. Mesoscale physical features, including open-ocean eddies, create ephemeral habitats with small-scale physical and chemical heterogeneity that has major consequences for microbial distributions and metabolic activities. This study shows that N_2-fixing cyanobacterial abundances in summer are highly variable relative to other important groups of microbes and are inextricably coupled to small-scale variations in nutrients caused by transport and mixing of water masses in the Station ALOHA region.

The projected increases in mesoscale activity in the region (Murakami *et al.*, 2013) should result in higher microbial patchiness at Station ALOHA, further complicating interpretations of station-based biogeochemical time-series data. A single short-term, high-resolution time series in this targeted region encountered a range of conditions comparable to years of summer sampling at Station ALOHA and showed that microbial distributions were clearly correlated with environmental factors. Monthly time-series programs that randomly sample open-ocean eddies show the same correlations over sustained, long-term sampling. Long-term changes in phosphate have been documented at Station ALOHA (Karl *et al.*, 2001), and recent studies have described a reversal of the long-term phosphate depletion in the region (Karl, 2014). We sampled on the cusp of this reversal in 2011 and our observations may reflect a corresponding regime change, which we would predict to be coupled with an increase in unicellular diazotrophs. On the basis of the current study, it appears that these types of nutrient changes directly affect diazotroph community composition that result in spatiotemporal changes in N_2 fixation. Given these characteristics along with their keystone species status, the importance of their biogeochemical function and the regularity with which they are quantified in the open ocean (Church *et al.*, 2005; Church *et al.*, 2008, 2009; Fong *et al.*, 2008; Moisander *et al.*, 2010), diazotroph populations can effectively serve as sentinel species for detecting ecosystem change.

Conflict of Interest

The authors declare no conflict of interest.

Acknowledgements

This work was funded by the MEGAMER facility grant by the Gordon and Betty Moore Foundation to JPZ, the David and Lucile Packard Foundation to CAS (through grants allocated to MBARI), the NSF Center for Microbial Oceanography, Research and Education (C-MORE grant number EF0424599) to JPZ and DMK, the Gordon and Betty Moore Foundation Marine Microbiology Investigator Program (JPZ and DMK), NSF grants OCE0425363 to JPZ and MJC, OCE0850827 to MJC (for historical *nifH* abundance measurements from Station ALOHA) and OCE0926766 to MJC and DMK (for support of the HOT program). Many thanks to Chris Edwards, Mariona Segura i Noguera, Ken Doggett, Susan Curless, Karin Björkman, Tara Clemente, Sara Thomas, Gene Massion, Kendra Turk, Ariel Rabines, Chris Preston, Nilo Alvarado, Brent Roman and Blake Watkins, and we are grateful for the expertise of the crew of the R/V *Kilo Moana*.

References

Ascani F, Richards KJ, Firing E, Grant S, Johnson KS, Jia Y *et al.* (2013). Physical and biological controls of nitrate concentrations in the upper subtropical North Pacific Ocean. *Deep-Sea Res II* **93**: 119–134.

Boyle EA, Bergquist BA, Kayser RA, Mahowald N. (2005). Iron, manganese, and lead at Hawaii Ocean Time-series Station ALOHA: Temporal variability and an intermediate water hydrothermal plume. *Geochim Cosmochim Acta* **69**: 933–952.

Carpenter EJ, Capone DG. (2008). Nitrogen fixation in the marine environment. In: Capone DG, Bronk DA, Mulholland MR, Carpenter EJ (eds), *Nitrogen in the Marine Environment*, 2nd edn. Academic Press: Burlington, MA, pp 141–198.

Church MJ, Björkman KM, Karl DM, Saito MA, Zehr JP. (2008). Regional distributions of nitrogen-fixing bacteria in the Pacific Ocean. *Limnol Oceanogr* **53**: 63–77.

Church MJ, Mahaffey C, Letelier RM, Lukas R, Zehr JP, Karl DM. (2009). Physical forcing of nitrogen fixation and diazotroph community structure in the North Pacific subtropical gyre. *Global Biogeochem Cycles* **23**: GB2020.

Church MJ, Short CM, Jenkins BD, Karl DM, Zehr JP. (2005). Temporal patterns of nitrogenase gene (*nifH*) expression in the oligotrophic North Pacific Ocean. *Appl Environ Microb* **71**: 5362–5370.

Davis CS, McGillicuddy DJ. (2006). Transatlantic abundance of the N_2-fixing colonial cyanobacterium Trichodesmium. *Science* **312**: 1517.

Dickey TD. (2003). Emerging ocean observations for interdisciplinary data assimilation systems. *J Mar Sys* **40-41**: 5–48.

Dore JE, Karl DM. (1996). Nitrification in the euphotic zone as a source for nitrite, nitrate, and nitrous oxide at Station ALOHA. *Limnol Oceanogr* **41**: 1619–1628.

Dore JE, Letelier RM, Church MJ, Lukas R, Karl DM. (2008). Summer phytoplankton blooms in the oligotrophic North Pacific Subtropical Gyre: Historical perspectives and recent observations. *Prog Oceanogr* **76**: 2–38.

Fong AA, Karl DM, Lukas R, Letelier RM, Zehr JP, Church MJ. (2008). Nitrogen fixation in an anticyclonic eddy in the oligotrophic North Pacific Ocean. *ISME J* **2**: 663–676.

Foster RA, Paytan A, Zehr J. (2009). Seasonality of N2 fixation and nifH gene diversity in the Gulf of Aquaba (Red Sea). *Limnol Oceanogr* **54**: 219–233.

Giovannoni SJ, Vergin KL. (2012). Seasonality in ocean microbial communities. *Science* **335**: 671–676.

Guidi L, Calil PHR, Duhamel S, Björkman KM, Doney SC *et al.* (2012). Does eddy-eddy interaction control surface phytoplankton distribution and carbon export in the North Pacific Subtropical Gyre? *J Geophys Res* **117**: 1–12.

Hashihama F, Furuya K, Kitajima S, Takeda S, Tekemura T *et al.* (2009). Macro-scale exhaustion of surface phosphate by dinitrogen fixation in the western North Pacific. *Geophys Res Lett* **36.**

Ilikchyan IN, McKay RML, Kutovaya OA, Condon R, Bullerjahn GS. (2010). Seasonal expression of the picocyanobacterial phosphonate transporter gene *phnD* in the Sargasso Sea. *Front Microbiol* **1**: 135.

Jackson JBC, Kirby MX, Berger WH, Bjorndal KA, Botsford LW, Bourque BJ *et al.* (2001). Historical overfishing and the recent collapse of coastal ecosystems. *Science* **293**: 629–638.

Johnson KS, Riser SC, Karl DM. (2010). Nitrate supply from deep to near-surface waters of the North Pacific subtropical gyre. *Nature* **465**: 1062–1065.

Karl DM. (2014). Microbially-mediated transformations of phosphorus in the sea: New views of an old cycle. *Ann Rev Mar Sci* **6**: in press.

Karl DM, Bjorkman KM, Dore JE, Fujieki L, Hebel DV, Houlihan T *et al.* (2001). Ecological nitrogen-to-phosphorus stoichiometry at Station ALOHA. *Deep-Sea Res Pt II* **48**: 1529–1566.

Karl DM, Church MJ, Dore JE, Letelier RM, Mahaffey C. (2012). Predictable and efficient carbon sequestration in the North Pacific Ocean supported by symbiotic nitrogen fixation. *Proc Natl Acad Sci USA* **109**: 1842–1849.

Karl DM, Tien G. (1992). MAGIC—a sensitive and precise method for measuring dissolved phosphorus in aquatic environments. *Limnol Oceanogr* **37**: 105–116.

Langlois RJ, Hummer D, LaRoche J. (2008). Abundances and distributions of the dominant *nifH* phylotypes in the Northern Atlantic Ocean. *Appl Environ Microb* **74**: 1922–1931.

Lehahn Y, d'Ovidio F, Lévy M, Heiftez E. (2007). Stirring of the northeast Atlantic spring bloom: A Lagrangian analysis based on multisatellite data. *J. Geophys Res* **112**: C08005.

Lukas R. (2001). Freshening of the upper thermocline in the North Pacific subtropical gyre associated with decadal changes of rainfall. *Geophys Res Lett* **28**: 3485–3488.

Lukas R, Santiago-Mandujano. (2008). Interannual to interdecadal salinity variations observed near Hawaii: local and remote forcing by surface freshwater fluxes. *Oceanography* **21**: 46–55.

Moisander PH, Beinart RA, Hewson I, White AE, Johnson KS, Carlson CA *et al.* (2010). Unicellular cyanobacterial distributions broaden the oceanic N_2 fixation domain. *Science* **327**: 1512–1514.

Murakami H, Wang B, Li T, Kitoh A. (2013). Projected increase in tropical cyclones near Hawaii. *Nat Climate Change* **3**: 749–754.

Ottesen EA, Young CR, Eppley JM, Ryan JP, Chavez FP, Scholin CA *et al.* (2013). Pattern and synchrony of gene expression among sympatric marine microbial populations. *Proc Natl Acad Sci USA* **110**: E488–E497.

Preston CM, Harris A, Ryan JP, Roman B, Marin R, Jensen S *et al.* (2011). Underwater application of quantitative PCR on an ocean mooring. *PLoS One* **6**: e22522.

Preston CM, Marin R, Jensen SD, Feldman J, Birch JM, Massion EI *et al.* (2009). Near real-time, autonomous detection of marine bacterioplankton on a coastal mooring in Monterey Bay, California, using rRNA-targeted DNA probes. *Environ Microbiol* **11**: 1168–1180.

Robidart JC, Preston CM, Paerl RW, Turk KA, Mosier AC, Francis CA *et al.* (2012). Seasonal *Synechococcus* and Thaumarchaeal population dynamics examined with high resolution with remote in situ instrumentation. *ISME J* **6**: 513–523.

Scholin CA. (2013). Ecogenomic sensors. In: Levin SA (ed.) *Encyclopedia of Biodiversity*, 2nd edn Volume 2. Academic Press: Waltham, MA 690–700.

Shilova IN, Robidart JC, Tripp HJ, Turk-Kubo K, Wawrick B, Thompson A *et al.* (2014). Development and application of a microarray for assessing gene transcription in open ocean microbial communities. *ISME J* in revision.

Shiozaki T, Kodama T, Kitajima S, Sato M, Furuya K. (2013). Advective transport of diazotrophs and importance of their nitrogen fixation on new primary production in the western Pacific warm pool. *Limnol Oceanogr* **58**: 49–60.

Sohm JA, Webb EA, Capone DG. (2011). Emerging patterns of marine nitrogen fixation. *Nat Rev Microbiol* **9**: 499–508.

Thompson AW, Foster RA, Krupke A, Carter BJ, Musat N, Vaulot D *et al.* (2012). Unicellular cyanobacterium symbiotic with a single-celled Eukaryotic alga. *Science* **337**: 1546–1550.

Westberry TK, Siegel DA. (2006). Spatial and temporal distribution of *Trichodesmium* blooms in the world's oceans. *Global Biogeochem Cycles* **20**: GB4016.

White AE, Spitz YH, Letelier RM. (2007). What factors are driving summer phytoplankton blooms in the North Pacific Subtropical Gyre? *J Geophys Res* **112**: C12006.

Wilson S, del Valle D, Robidart J, Zehr J, Karl D. (2013). Dissolved hydrogen and nitrogen fixation in the oligotrophic North Pacific Subtropical Gyre. *Environ Microbiol Reports* **5**: 697–704.

Zehr JP, Montoya JP, Jenkins BD, Hewson I, Mondragon E, Short CM *et al.* (2007). Experiments linking nitrogenase gene expression to nitrogen fixation in the North Pacific subtropical gyre. *Limnol Oceanogr* **52**: 169–183.

Zehr JP, Robidart J, Scholin C. (2011). Marine microbes, biogeochemical cycles, and global climate change. *Microbe* **6**: 169–175.

Supplementary Information accompanies this paper on The ISME Journal website (http://www.nature.com/ismej)